Molecular Psychiatry (2017) 22, 1230–1240
www.nature.com/mp

OPEN

EXPERT REVIEW

Connectome imaging for mapping human brain pathways

Y Shi and AW Toga

With the fast advance of connectome imaging techniques, we have the opportunity of mapping the human brain pathways *in vivo* at unprecedented resolution. In this article we review the current developments of diffusion magnetic resonance imaging (MRI) for the reconstruction of anatomical pathways in connectome studies. We first introduce the background of diffusion MRI with an emphasis on the technical advances and challenges in state-of-the-art multi-shell acquisition schemes used in the Human Connectome Project. Characterization of the microstructural environment in the human brain is discussed from the tensor model to the general fiber orientation distribution (FOD) models that can resolve crossing fibers in each voxel of the image. Using FOD-based tractography, we describe novel methods for fiber bundle reconstruction and graph-based connectivity analysis. Building upon these novel developments, there have already been successful applications of connectome imaging techniques in reconstructing challenging brain pathways. Examples including retinofugal and brainstem pathways will be reviewed. Finally, we discuss future directions in connectome imaging and its interaction with other aspects of brain imaging research.

Molecular Psychiatry (2017) **22,** 1230–1240; doi:10.1038/mp.2017.92; published online 2 May 2017

INTRODUCTION

Mapping the connectivity of brain circuits is fundamentally important for our understanding of the functions of human brain. Various neurological and mental disorders have been linked to the disruption of brain connectivity in circuits such as the cortico–striato–thalamo–cortical network,[1–3] reward circuits[4] and limbic system.[5] Tracer injection studies have been historically utilized for this mapping and continue to be the most reliable way of inferring axonal connection in mammalian brains,[3,6] but their usability is limited to animal studies. For *in vivo* mapping of human brain connectivity, magnetic resonance imaging (MRI) is the most powerful modality with its non-invasive nature and versatility in examining both the structure and function of the brain.

There are two main modalities for studying brain connectivity with MRI: diffusion and functional MRI (fMRI). Diffusion MRI (dMRI) collects signals that are sensitive to the diffusion of water molecules along different directions.[7,8] dMRI data can be used to compute the probabilistic distribution of axonal orientations, which are then concatenated to establish structural connectivity across brain regions with tractography techniques.[9,10] fMRI measures the fluctuation of blood-oxygen level dependent (BOLD) signals and establishes connectivity as the synchronization of fMRI signals at different brain locations.[11–13] Since the invention of both techniques two decades ago, tremendous progress has been made both technologically and scientifically, which culminated in the funding of the Human Connectome Project (HCP: http://www.humanconnectomeproject.org/) by NIH in 2009.[14,15] In particular, we have witnessed over the last few years the dramatic advances and maturation of multiband imaging techniques and their adoption in connectome imaging protocols.[16–18] This has resulted in almost two orders of magnitude increase of imaging data with much improved resolution spanning the spatial, temporal and angular dimensions.[19–21]

These rich resources in connectome imaging present great opportunities to map human brain pathways at unprecedented accuracy. On the other hand, this avalanche of BIG DATA[22,23] in connectomics[24,25] also poses challenges for existing image analysis algorithms. This has stimulated the development of novel analytic solutions for studying brain connectivity in various aspects of connectome imaging. In this article, we focus on the review of recent progresses of connectome imaging with dMRI methods. We first introduce the basic concepts of diffusion imaging and related techniques for modeling brain microstructure. We also discuss the tractography techniques and how they can be used to reconstruct fiber bundles and study network connectivity. Finally, future research directions in connectome imaging and their application in neuroscientific research are presented.

BACKGROUND OF DIFFUSION IMAGING

Understanding the diffusion imaging signal

In a dMRI experiment, the data we collect are a series of 3D volumes. Among these volumes, some of them, called B0 images, are generated without the application of diffusion gradients. The rest of the images are acquired with varying diffusion gradients that are useful for characterizing axons in different spatial arrangements. As summarized in Table 1, key parameters in dMRI experiments include diffusion time, gradient strength and gradient directions.[26,27] In principle, the diffusion signal is from the dephasing of the spins due to their displacement during a dMRI experiment. The diffusion time determines probabilistically how far the distance the water molecules, or the spins, will travel in a dMRI experiment. With the increase of the diffusion time, the spins will likely travel farther away from their original location and thus result in more attenuation in

Laboratory of Neuro Imaging (LONI), USC Stevens Neuroimaging and Informatics Institute, Keck School of Medicine, University of Southern California, Los Angeles, CA, USA. Correspondence: Dr AW Toga, Laboratory of Neuro Imaging (LONI), USC Stevens Neuroimaging and Informatics Institute, Keck School of Medicine, University of Southern California, 2025 Zonal Avenue, Los Angeles, CA 90032, USA.
E-mail: toga@loni.usc.edu
Received 9 December 2016; revised 6 February 2017; accepted 24 February 2017; published online 2 May 2017

Table 1. Some key parameters in diffusion imaging

Diffusion time Δ	Longer Δ results in more attenuation in diffusion signal
Gradient strength G	Stronger G results in more attenuation in diffusion signal
b-value $b = (\gamma\delta G)^2(\Delta - \frac{\delta}{3})$	Summarizes the effect of gradient strength and diffusion time, where γ is the gyromagnetic ratio (a constant) and δ is the duration of gradient encoding
Single-shell dMRI	Varying gradient directions with a fixed b-value
Multi-shell dMRI	Varying gradient directions with a small set of b-values. Three different b-values were used in HCP protocol

Abbreviations: dMRI, diffusion MRI; HCP, Human Connectome Project.

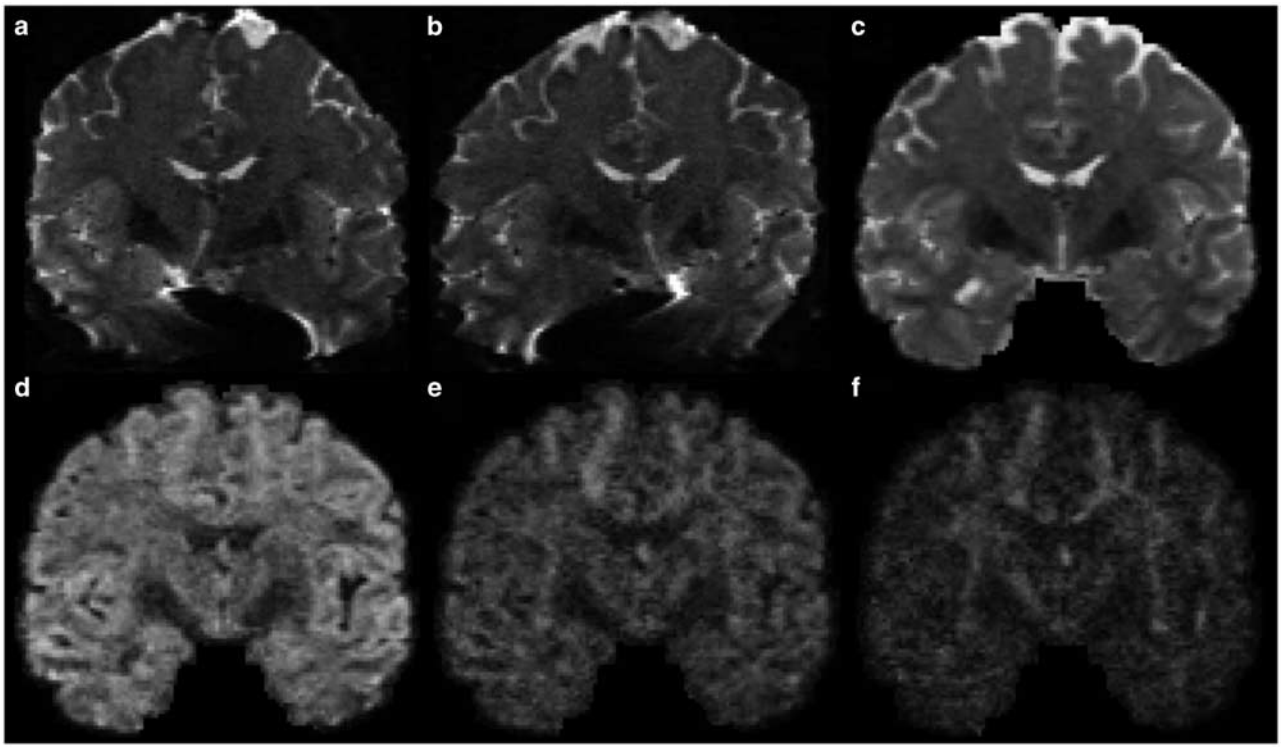

Figure 1. Multi-shell diffusion imaging from the Human Connectome Project. B0 images from L/R phase encoding (**a**) and R/L phase encoding (**b**) show the images were distorted in opposite phase encoding directions due to susceptibility in the magnetic field. (**c**) Corrected B0 image after removing susceptibility-induced distortion and merging the data from L/R and R/L phase encodings. Multi-shell diffusion imaging acquires data from several b-values. For the gradient directions along the x axis, the images from $b = 1000, 2000, 3000$ s mm^{-2} are shown in (**d**–**f**), respectively. Note the greater attenuation in the image intensity with an increased b-value.

the MR signal. Besides the diffusion time, the gradient strength also affects the diffusion signal. The stronger the gradient strength, the more attenuation we have in the dMRI image. The effect of both diffusion time and gradient strength is summarized in the quantity called b-value. In conventional dMRI experiments, the b-value is fixed and only the gradient directions were changed to acquire a series of 3D volumes. This is the so-called single-shell Q-ball acquisition[28] in contrast to the multi-shell acquisition scheme (Figures 1d–f) used in the connectome imaging protocols.[20] In multi-shell experiments, a small set of different b-values is used in addition to the change of gradient directions. This provides an opportunity of more sophisticated modeling of water diffusion in human brain. More generally, we can have a different b-value for each gradient direction. This is the acquisition scheme adopted in the diffusion spectrum imaging.[29] By fully sampling the q-space, diffusion spectrum imaging can theoretically recover the diffusion profile at each voxel, but it faces the challenges of long scan time and low signal to noise at high b-values.

Artifacts in diffusion imaging

The main artifacts in diffusion imaging include head motion, eddy currents[30] and susceptibility-induced distortion.[31] Head motion and eddy currents lead to misalignment of brain regions across image volumes acquired with different gradient directions. These two types of artifacts are global in nature, so they are typically corrected in the same framework with image registration methods.[32] The challenge, however, is the dramatic change of image signals with the variation of gradient directions. Early works relied on registration to the B0 images by modeling the head motion and eddy currents as affine transformations.[30] With the availability of data from densely sampled gradient direction, more sophisticated models that rely on the prediction of the signals from neighboring gradient directions were developed.[33] Under this framework, polynomial transformations can be applied to achieve improved performance in correcting distortions from eddy currents.[34]

Susceptibility-induced distortion is due to the inhomogeneity in the magnetic field. It is subject dependent, so every brain scan can have varying degrees of distortion. It is most severe in regions

with a tissue–air boundary such as the orbital frontal cortex or brainstem, so the distortion field is inherently local. Susceptibility-induced distortion not only distorts the brain image, but also results in the loss of signals. This is caused by the piling up of signals from multiple voxels into a single voxel. To correct for susceptibility-induced distortion, early work relied on the measurement of a field map and used that to correct for the geometric distortion,[35] but this method is time consuming and cannot reverse the signal loss due to piling up of signals. More recently, methods based on collecting two copies of dMRI data with opposite phase encodings were developed (Figures 1a–c).[36–38] This approach is based on the observation that the distortions from opposite phase encodings mirror each other. Technically this is also feasible with the dramatic increase of acquisition speed in the connectome imaging protocol. Compared with corrections based on field maps, better correction has been achieved with data from opposite phase encodings.[37]

Besides the artifacts mentioned above, other subtler artifacts such as bulk motion from cardiac pulsation are receiving more attention.[39] The bulk motion from pulsation can cause the loss of diffusion signal in regions such as the brainstem. Cardiac gating has been proposed,[40,41] but it leads to a reduction of acquisition speed. For connectome imaging data, automated algorithms have been proposed recently to identify voxels with such artifacts and alter their numbers with predicted values from uncorrupted signals.[42]

MICROSTRUCTURAL MODELS

Besides the MRI parameters such as diffusion time and gradient strength, the local microstructure of the brain also affects the diffusion imaging signal. For spins inside the myelinated axons, their diffusion is restricted in the transverse direction. For spins outside the axons, their diffusion is hindered by the surrounding cellular environment, which includes the walls of the axons.[43] With dMRI data, our goal is to quantitatively characterize the microstructure of brain tissues and detect changes due to pathology.

Tensor models

To model the distribution of spins using the dMRI data, the Gaussian distribution was first proposed.[7,8] The tensor matrix in the Gaussian model is symmetric and contains six parameters. This model only needs six diffusion-weighted images, so the data acquisition can be conducted fairly efficiently on 1.5T MRI scanners, which was highly desirable in the early stages of dMRI. For the robust estimation of the tensor, data from more gradient directions are typically acquired that range from 12 to 30 directions. Various numerical algorithms have been developed to estimate the tensor from dMRI data that ranges from direct least square fitting[44] to more sophisticated approaches that ensure the non-negativity of the tensor matrix.[45] Since its emergence, the tensor model has been used widely in various brain imaging studies. Presently, the term diffusion tensor imaging (DTI) is almost synonymous with diffusion imaging even though the field has advanced dramatically beyond the tensor models.

The eigen structure of the tensor model provides some of the most popular features in connectivity studies.[46] Since the tensor is a 3×3 matrix, it has three eigenvalues and associated eigenvectors. The largest eigenvalue is called the axial diffusivity, the mean value of the other two eigenvalues defines the radial diffusivities. These definitions reflect our desire to model the diffusion of spins along axons as elongated ellipsoids. Using these three eigenvalues, the fractional anisotropy (FA) is defined to characterize the anisotropy of the underlying diffusion. The FA can take values between 0 and 1. The FA is 0 when the tensor is purely isotropic, that is, the three eigenvalues are equal. The FA increases when the tensor becomes more elongated, that is, the water diffusion is more anisotropic. It reaches the value 1 when the tensor is a stick model with zero radial diffusivity.

The diffusivity measures are highly sensitive measures for the detection of microstructural changes. They have been applied in studying various neurological[47–49] and mental disorders.[50,51] Extra caution must be taken when interpreting these measures because multiple pathological events can lead to very similar changes in the diffusivity. This lack of specificity is one of the well-known limitations of diffusion imaging. While there were efforts that tried to separate the contributions of demyelination, axonal transection and edema,[52,53] significant research still needs to be done to translate such research into human studies.

High-order tensors and tensor mixtures

For the modeling of the anisotropy in water diffusion, the tensor model is most suitable for locations where there is only one fiber direction. When there are more complicated configurations including fanning and crossing of fibers, we need more advanced data acquisition schemes and mathematical models. From the data acquisition perspective, high-angular resolution diffusion imaging that collects data from a large number (60–100) of gradient directions at the same *b*-value has been helpful.[28,54] This motivates the development of more sophisticated modeling algorithms to better characterize the water diffusion from a complicated fiber architecture.

Similar to the Gaussian mixture model in statistics, the mixture of the tensor models[55,56] is a natural extension of the tensor to characterize the high-angular resolution diffusion imaging signal. There are several challenges, however, in this approach. First is the need to select the number of the components. If very few components are selected, we might miss important fiber directions and fail to properly characterize the dMRI signal. On the other hand, numerical problems can arise if too many components are used since the extra components might be forced to fit the noise in the dMRI signal. Because the complexity of the fiber architecture varies across different brain regions, it is impractical to fix the number of the components. The second challenge of the tensor mixture model is the nonlinearity of the optimization problem. In contrast to the tensor model, the optimization of the tensor mixture model is highly nonlinear, which means we might encounter local optima frequently. This is especially challenging given the possibility that the extra tensor components can fit the noise. To alleviate this difficulty, Monte Carlo sampling and information-theoretic model selection were adopted.[55]

Fiber orientation distribution

Fiber orientation distribution (FOD)[57,58] is a non-negative function defined on the unit sphere with its values representing the probability of fiber tracts along each direction (Figure 2a). It is related but different from orientation distribution function, which is computed with a series of approximation steps in q-ball imaging.[59] Compared with the tensor mixture models, FOD has the flexibility in representing arbitrary fiber configurations without the need of specifying the number of fiber crossings *a priori*. The numerical solution of FOD is also more tractable as it typically consists of deconvolution steps that are quadratic or convex.[57,58,60,61–63] For these reasons, FOD is becoming increasingly popular and emerging as a standard representation of fiber connectivity.

Numerically the FOD is represented as a linear combination of spherical harmonics.[65] Most existing tools for computing FODs were developed for single-shell dMRI data. The multi-shell imaging data from HCP have motivated the development of

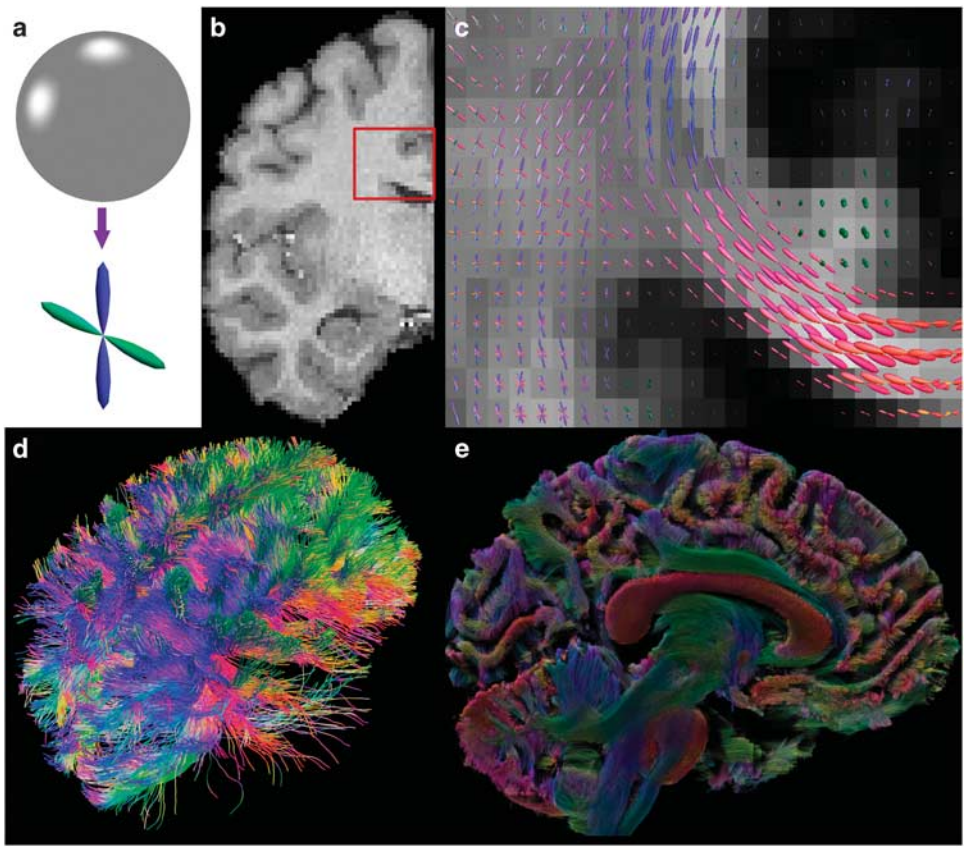

Figure 2. An illustration of fiber orientation distribution (FOD) reconstructed from Human Connectome Project (HCP) data with the method we developed recently.[64] (**a**) FOD is a function on the unit sphere (top) and can be visualized as a 3D shape (bottom) by modulating the radius of the shape according to the magnitude of the FOD function. For an region of interest (ROI) shown as the red box in (**b**), the FODs are visualized in (**c**). (**d**) With FOD-based tractography, a more complete representation of the corpus callosum can be reconstructed. The lateral projections of the corpus callosum were successfully captured. As shown in (**e**), a volume rendering can be created with 3 million fiber tracts to visualize the connectome of the human brain.

novel FOD reconstruction algorithms.[64,66–70] With the multi-shell and high-angular resolution data from HCP, we can estimate FODs with high-order spherical harmonics.[64] This generates very-sharp FODs that will improve the resolution of crossing fibers at each voxel, which will no doubt assist the tractography algorithms for brain connectivity modeling (Figure 2). Besides FOD estimation, the multi-shell HCP data have enabled the incorporation of compartment modeling[43,71] into the estimation of FODs.[64] These compartment parameters provide novel measures about the integrity of white matter microstructure. The compartment models also improve the robustness of FOD estimation in regions with complicated tissue compositions such as the thalamus and gray matter/white matter boundaries.

TRACTOGRAPHY-BASED MAPPING OF BRAIN PATHWAYS

Tractography methods

While there are many exciting advances in sophisticated tractography algorithms,[72–74] the streamline approach is still the most widely applied method for fiber tractography using tensor or FODs.[9,10,75] Intuitively, we can imagine this tractography algorithm is simulating the movement of a water molecule along the axons. The starting position of this tracking process is called a seed point. At each point of the tracking process, we utilize the FOD or tensor at the current location to generate the next direction to extend the tract. The water molecule is then moved along this direction for a specific distance, which is called the step size. The process is repeated until a stopping criterion is satisfied. The tract is accepted if it meets certain anatomical requirements that are typically problem specific.

There are several key factors that affect the results of fiber tractography. The first factor is the anatomical protocol that we prescribe to determine if a fiber tract is valid. This represents the anatomical knowledge we have about the specific circuits under study. Practically, they are represented as the regions of interest (ROIs) that a fiber tract needs to pass or avoid. The second factor is the overall shape of the fiber tract has to be biologically plausible. Overall a smooth trajectory is expected. This is controlled by a combination of several parameters including the step size and maximum turning angle at each step. The third factor is how we generate the movement direction at each step. This is where the deterministic and probabilistic tractography deviate from each other.[55,75] For deterministic tractography, the peak direction of the tensor or FOD is selected. Since FODs have multiple peaks, one of them, typically the direction with the smallest angle with the incoming direction, will be selected. For probabilistic tractography, we view the FOD or tensor as mathematical representations of the probabilistic distribution of fiber directions. To obtain the next direction to move the water molecule, a stochastic procedure is run to draw a sample direction from this distribution. For each direction, the chance of it being selected is in proportion to its magnitude in the probabilistic distribution. This direction is accepted if it satisfies the shape constraints.

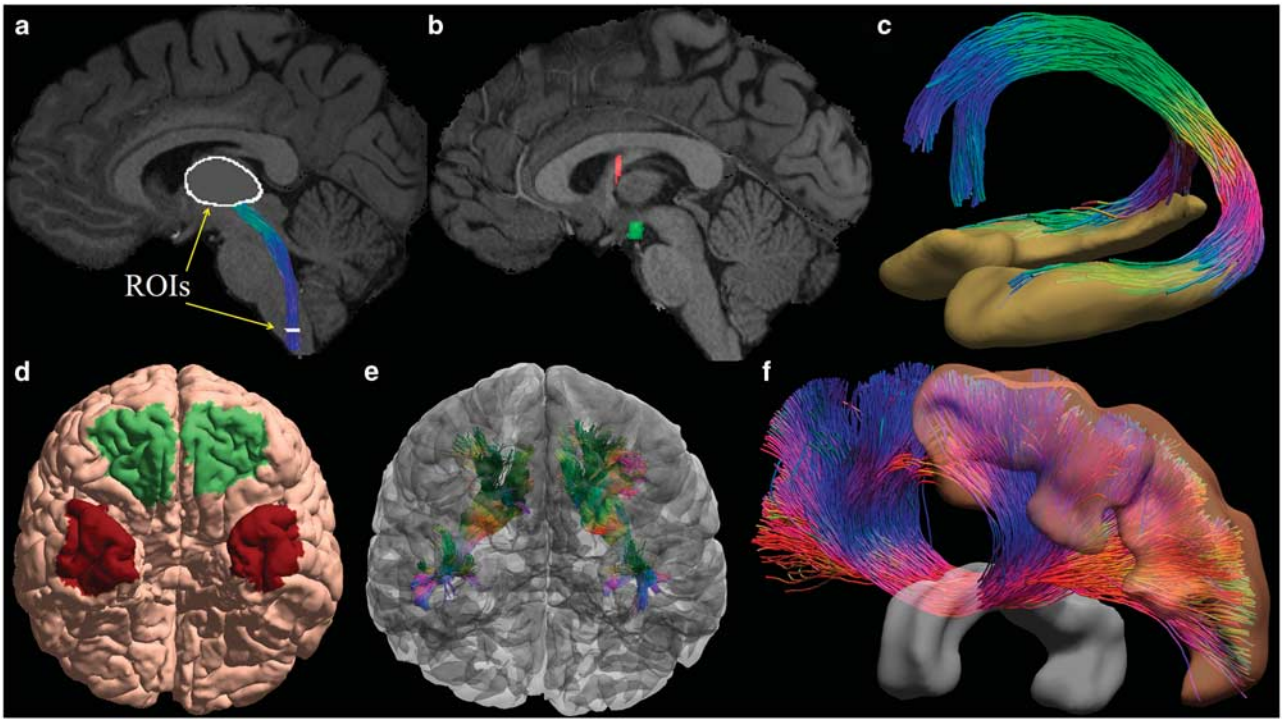

Figure 3. With connectome imaging data, we can more accurately reconstruct human brain pathways using fiber orientation distribution (FOD)-based tractography and anatomical region of interests (ROIs). (**a**) ROIs in the medulla and thalamus were used to reconstruct the spinothalamic pathway. (**b**) For the reconstruction of the fornix bundle, we use multiple ROIs including the hippocampus, a fornix ROI, mammillary body and basal forebrain. Here two of the ROIs were plotted: red: fornix; green: mammillary body. (**c**) The reconstructed fornix bundle is overlaid with the hippocampal surfaces. Note that two branches to the mammillary body (posterior branch) and the basal forebrain (anterior branch) have been successfully reconstructed. (**d**) Surface-based ROIs were used for the reconstruction of the uncinated fasciculus. Green: orbital frontal cortex; Red: anterior temporal cortex. (**e**) The reconstructed uncinated fasciculi on both hemispheres are overlaid with the cortical surfaces. (**f**) Corpus callosum bundle connecting the precentral gyrus (motor cortex) of both hemispheres has been reconstructed with ROIs including the precentral gyrus and the middle sagittal corpus callosum ROI. Both ROIs are rendered as 3D surfaces in this plot.

Fiber bundle reconstruction

One main application of tractography is reconstructing a digital representation of major white matter bundles (Figure 3). This is achieved via a carefully designed anatomical protocol including a set of AND ROIs that a fiber tract should pass and a set of NOT ROIs that the fiber tract should not touch.[76–78] Because the number of AND ROIs is typically small (2–3), we need the NOT ROIs to add more control over the trajectory of the fiber bundle. In early studies, the ROIs were manually drawn on anatomical MRI images. This approach is time consuming and can only be conducted in studies with small sample sizes. For large-scale studies such as the HCP, we need to develop automated algorithms that can leverage the recent development in brain image analysis algorithms. Using software tools such as FreeSurfer[79] and FSL,[80] we can extract a set of generic cortical and sub-cortical ROIs, but this is usually not enough. For additional ROIs that are needed for specific bundles, the label fusion framework[81–83] provides a general strategy for automated volumetric ROI segmentation, which we have also extended to surface ROIs.[84] This entails the manual delineation of the necessary ROIs on a set of representative subjects. After that, these masks are warped to the image space of new subjects with a non-linear registration software tool.[85] The ROIs of the new subjects are finally formed via the fusion of these warped ROIs based on a weighted voting process. The general workflow can be applied to both gray matter and white matter regions. For challenging situations where there is a lack of visible contrast in available MRIs for manual segmentation, innovative strategies must be developed. For example, a combination of contextual information from surrounding nuclei and the continuity of the retinofugal tracts in the digital space were proposed to automatically define the lateral geniculate nuclei for the reconstruction of the optical radiation.[86]

Even with the constraint of multiple ROIs, it is common for the reconstructed fiber bundle to contain outlier tracts. Possible causes include the complexity of the anatomy, too much freedom in probabilistic tractography or noise in the estimated FODs. For small-scale studies, manual editing can be applied to remove the outliers in the bundles. For large-scale studies, various automated filtering strategies have been developed. Intuitively we have two ways to identify outlier tracts. The first approach is based on the observation that outlier tracts tend to be far away from the 'main' bundle. Mathematically this can be captured as distance measures between fiber tracts differential geometry. Using the pairwise distances between tracts, a spectral clustering technique can be applied to divide the fiber tracts into clusters of tracts.[87] After that, small clusters can be removed as outliers. This has been successfully applied in various fiber bundle clustering projects.[88] The difficulty with this approach is the lack of intuition in tuning the parameters for the spectral clustering. For individual bundles, a fine tuning process is needed to find the optimal parameters for large-scale application. The second possible approach for identifying outliers is based on the density of fiber tracts. This assumes that outliers are more scattered in space and they have lower density than the main bundle. To implement this idea numerically, we can convert the fiber tracts into a tract density image[89] and then remove the outliers following thresholding the tract density image. On the basis of the tract density image representation of fiber bundles, topological analysis strategies can also be

developed to remove the outliers.[90] For large-scale brain imaging studies, a successful reconstruction of fiber bundles might need a combination of multiple tract filtering approaches since each of them captures a somewhat different aspect of outlier tracts.

Graph-based modeling

Using fiber tractography, we can also build network models of brain connectomes[91] and apply graph-based measures to study connectivity.[92,93] There are two main steps in conducting network studies in brain imaging. The first step is graph construction and the second step is the calculation of various network measures.

A graph is composed of a set of nodes and edges. Two nodes are connected if there is an edge between them. To define the nodes for brain connectomes, various approaches have been proposed to parcellate the brain into many smaller regions. A popular choice is to use cortical labels produced from software tools such as FreeSurfer[79] or warping an atlas with cortical labels, such as the LPBA40 atlas,[94] to the subject space. More fine-grained parcellation can be obtained by further dividing these regions.[91] These parcellations, based on structural MRIs, can be further improved with multimodal information. Recent results from HCP suggest that a detailed parcellation can be obtained using functional connectivity patterns,[95] but it relies on manual interaction. Overall, the definition of nodes in connectome studies is still an open question that needs further technical and scientific investigations. Once we have a set of nodes, we can define the edges using fiber tractography, which could be weighted or unweighted. If there are fiber tracts connecting two ROIs, we can define the connectivity using quantities such as the number of tracts, mean values of diffusivity and FA. By thresholding the weights on the edges, we can also obtain a binary graph where the weight on an edge is either 1 (connected) or 0 (unconnected).

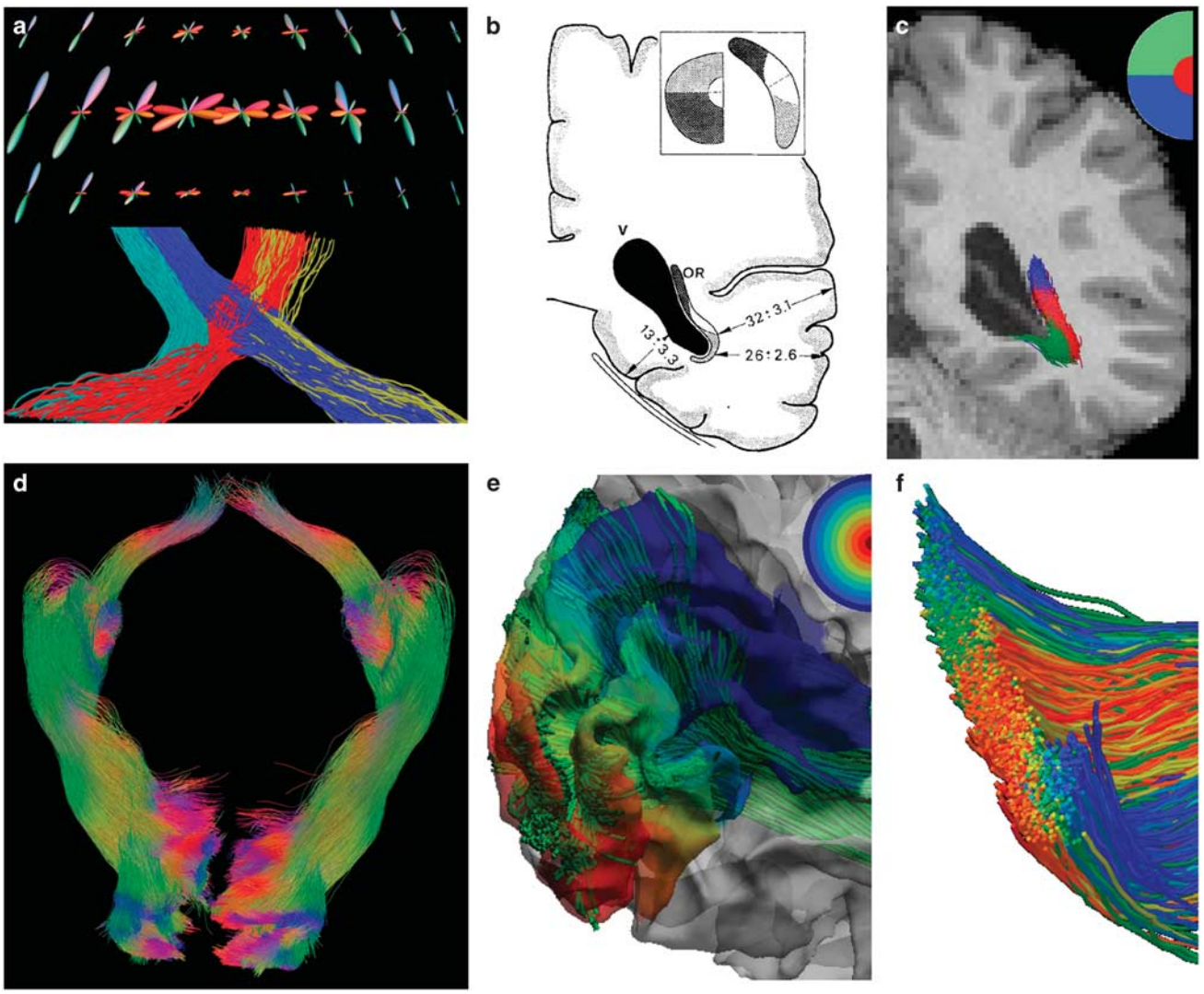

Figure 4. Retinofugal visual pathway reconstruction results. (**a**) Top: fiber orientation distributions (FODs) at the optic chiasm; Bottom: the ipsilateral and contralateral branches of the optic tracts were reconstructed from the FODs. Reconstructed fiber bundles from an Human Connectome Project (HCP) subject. (**b**) Postmortem dissection result[99] shows the retinotopic organization of the optic radiation. (**c**) Retinotopic parcellation of the left optic radiation fiber bundle reconstructed by our method as shown in (**a**). Red, blue, green represent fiber projecting to the foveal, superior and inferior quadrant of the peripheral visual field, respectively. (**d**) The reconstructed retinofugal pathways including the optic tract and optic radiation of both hemispheres. (**e**) Using the cortical projection of the visual pathway, detailed retinotopic coordinates (eccentricity, angle) can be assigned to each fiber tract. Here the eccentricity map is plotted as a colored map on the cortex. (**f**) A cross section of the optic radiation bundle with tracts colored by the eccentricity as defined through their projection onto V1.

Once the graph construction is completed, a matrix representation can be generated where each entry records the edge weight of corresponding node pairs denoted by the row and column index of the matrix. Basic measures such as the degree of nodes and shortest path can be computed easily from the matrix representation. More advanced measures such as characteristic path length and clustering coefficients can then be derived from these basic measures.[25,96] On the basis of these measures, small-worldness can be defined,[92] which compares the clustering of nodes and their distances to random graphs. More recently, quantitative measures for hubs and rich clubs were proposed and successfully applied to imaging studies of psychiatry studies.[97] Together with fiber bundles for specific circuits, network measures are valuable to provide complementary, global characterizations about the connectivity of brain networks.

APPLICATION OF CONNECTOME IMAGING IN MAPPING BRAIN PATHWAYS

With the high-resolution data from connectome imaging, we have the opportunity to extend the reconstruction of human brain pathways with increased completeness and capturing more fine-grained details. While these high-quality connectome imaging data of HCP are only available recently, there have already been active research efforts in utilizing them to reconstruct pathways that were difficult to achieve with conventional diffusion imaging techniques. Here, we review the progress of these early studies in the reconstruction of visual pathways, brainstem pathways and language pathways. Because the application of the HCP connectome imaging protocol in psychiatry studies has been limited to date, we provide these examples to demonstrate the utility of brain pathway reconstruction with cutting-edge MRI methods. This hopefully will motivate rapid adoption of the connectome imaging protocol in future psychiatry studies.

Visual pathways

The retinofugal pathways include the optic nerves, optic chiasm, optic tracts, lateral geniculate nuclei and the optic radiation. While various methods were proposed to reconstruct these important pathways with dMRI, the unique complexities of the visual pathway have impeded the development of a robust and automated reconstruction method with tractography. The difficulties include the crossing fibers at the chiasm, the tortuous course of Meyer's loop, proximity to multiple neighboring fiber bundles and limited contrast of the lateral geniculate nucleus in structural MRIs. We have developed an automated system for the reconstruction of the retinofugal visual pathway from optic chiasm to the primary visual cortex[86] and the corpus callosum. With HCP data, our group has developed an automated system to overcome these challenges. The ultra-sharp FODs computed by our method from HCP data greatly enhance our ability to capture Meyer's loop in the temporal stem where multiple major fiber bundles cross.[98] Our system also automatically identifies related anatomical ROIs including the lateral geniculate nucleus and primary visual cortex (V1), and reconstructs anatomically faithful representations of the visual pathway. As shown in Figure 4, the sharp FODs from our method are able to generate highly organized fiber tracts that follow the retinotopic organization of the visual pathway. Quantitative measurements also show that our results achieve excellent agreement with postmortem dissection studies[99] and the Contrack method,[100] a DTI study based on manual intervention. Using reconstructed bundles of the 215 HCP subjects, we also found a statistically significant leftward asymmetry of the optic radiation volume that is consistent with postmortem studies.[101]

Brainstem pathways

The brainstem regulates vital and autonomic functions, relays motor and sensory information between the brain and peripheral nervous system, and modulates cognition, mood and emotions.[102,103] Fiber pathways from brainstem nuclei innervate extensive cortical and sub-cortical regions and play important modulatory roles in various cognitive and behavioral functions.[104] Due to the complexity of brainstem anatomy and limited resolution of conventional dMRI, it has been a challenge to reliably map the brainstem pathways. With the much improved resolution from connectome imaging techniques, there has been growing interest in studying the brainstem-related pathways. Using an averaged data set created from 488 HCP subjects, a comprehensive set of brainstem pathways was reconstructed.[105] The validity of the trajectories of the reconstruction results was compared with histology images of five postmortem brains at various sections of the brainstem. A probabilistic atlas of cerebellar peduncles was also developed recently with data from 90 HCP subjects.[106] The inferior, middle and superior cerebellar peduncles were reconstructed from each brain and aligned to create the probabilistic atlas. For the *in vivo* reconstruction of the pathways in the homeostatic network of human brains,[107] high-resolution diffusion spectrum imaging data were collected with the MGH-USC Connectome scanner that has $300\,\mathrm{mT\,m^{-1}}$ maximum gradient strengths and a 64-channel coil. The 55 min diffusion spectrum imaging protocol included 515 q-space samples, and its maximum *b*-value is $10\,000\,\mathrm{s\,mm^{-2}}$. With this data set, a central homeostatic network between six brainstem nuclei and seven forebrain regions was reconstructed. The connectivity matrix was formed by counting streamline probability between each pair of brainstem and forebrain regions. Detailed examination of the fiber tracts was conducted and branches of the medical forebrain bundles, and a lateral forebrain bundle from brainstem to medial temporal lobe were identified.

Language pathways

The superior longitudinal fasciculus (SLF) and arcuate fasciculus (AF) are important components of the language networks. The exact pathways of these two fiber systems, however, are still under debate in previous DTI studies. While some DTI studies considered the AF as composed of the ventral and dorsal segments,[108] others classified the most ventral segment of SLF (SLF III) as part of indirect segments of AF.[109] By comparing the tractography reconstruction of HCP data with the dissection results of 25 postmortem brains, the detailed pathways of the SLF and AF were examined by Yagmurlu *et al*.[110] Three SLF segments (dorsal SLF I, middle SLF II and ventral SLF III segments) and two AF segments (ventral and dorsal) were robustly reconstructed on both dissection and tractography reconstruction. In particular, the topographic relation of the AF pathways and the SLF3 segments were clearly identified.

These results provided a glimpse of the possibility with connectome imaging data for improving the state-of-the-art in fiber pathway reconstruction. Overall, we can see more faithful characterization of brain anatomy could be achieved with careful application of the connectome image techniques. With the wider application of these methods to other under-explored brain regions, it is anticipated more exciting progress will be made in the coming years.

FUTURE DIRECTIONS

The connectome imaging techniques represent a leap in brain imaging capabilities that provide a whole new paradigm for studying human brains *in vivo*. While great advances have been achieved in the last decade, this is a fast moving field and we anticipate major advances in the following areas.

Continued improvement in imaging technology

Current connectome imaging protocols have already achieved more than one order of magnitude speed up in acquiring diffusion and fMRI data. However, the relative long acquisition time of the full HCP protocol poses serious challenges for their adoption in disease studies. Even with the state-of-the-art 3T MRI scanners, only a portion of the HCP protocol can be included in disease studies. There is thus a great need to further optimize imaging protocols for multiple time frames suitable for imaging research and clinical applications. Continued research in multiband and parallel imaging techniques will no doubt help in this aspect. Optimization of existing connectome protocols for a given time frame should also be investigated, where the challenge is the definition of a gold standard for the trade-off between spatial resolution, number of gradient directions and distribution of *b*-values. In our current research, we find that the retinotopic organization of the visual pathway provides an ideal test bed for the *in vivo* validation of tractography techniques.[111] There are other brain regions that also have well-characterized anatomy such as the cortical–striatum connections.[3] These can serve as valuable resources for quantification of the performance of different acquisition schemes. The extension of connectome imaging to 7T MRI is another exciting direction.[112] Major advances have been achieved for 7T diffusion and function MRI acquisition in HCP. In principle, 7T MRI will provide higher signal to noise and improved resolution, thus there is a great opportunity for more fine-grained mapping of brain pathways. Besides advances in image acquisition, we will witness continued research and improvement in image processing algorithms. Novel preprocessing methods will help the correction of imaging artifacts such as eddy current and susceptibility distortion, and signal dropout due to bulk movement. The fusion of data from multiple phase encodings also needs more dedicated research to improve signal quality for connectome modeling. Innovations in post-processing algorithms will lead to better tractography algorithms that can more faithfully represent brain anatomy such as the topographic organization fiber bundles.[111] Compartment modeling has the potential of separating intra- and extra axonal changes in tissue microstructure.[43,113–115] More sophisticated algorithms in compartment modeling, such as the NODDI model,[116] could provide novel opportunities for improving the specificity in the characterization of connectivity changes.

Validation of microstructure and tractography methods

One fundamental question in connectome imaging is the validation of the digital connectivity from MRI data. While it is generally difficult to obtain ground truth about human brain connections, detailed anatomical knowledge is available for certain pathways that can be used to quantitatively evaluate the performance of tractography methods. One particular example is the topographic organization of sensory pathways such as the retinotopic organization of the visual pathway[117] and the somatotopic organization of the somatosensory pathway.[118] Such topographic organization provides an ideal opportunity for examining the pathway integrity at specific locations when the topographic location of atrophy is known from separate measurements such as retinal imaging. More generally, animal tracing studies provide the ground truth about brain connectivity, but the number of injection sites were usually limited.[119–121] For mouse brain tracing studies, tremendous progress has been made with the creation of detailed connectomes with whole-brain coverage.[6,122] These are highly valuable resources for examining the performance of tractography algorithms.[123,124] Such validation experiments will improve our understanding about the impact of model selection and various parameters in tractography. For postmortem tissues, immunohistochemistry-based staining will provide valuable information for the validation of compartment models.[125] By measuring myelin content and the volume of extra axonal cellular structures, we can quantify the agreement between compartment models and tissue compositions. Overall there is a great need to validate the cutting-edge connectome imaging methods and we believe this need will be met with additional validation studies using biological ground truth. While these validation experiments using postmortem samples are critical, their translation to *in vivo* studies should also be carefully investigated. This could be achieved with carefully designed and streamlined experiments that include *in vivo* MRI, tracer injections and postmortem MRI, and measurement from immune histology. To carry out these sophisticated experiments and data analysis, it is important to foster the collaboration between multidisciplinary teams with complimentary expertise.

Multimodal connectivity fusion

The functional connectivity from resting fMRI is mainly derived from the correlation of the BOLD signal in gray matter regions. Tractography methods are capable of mapping pathways across white matter regions. In principle, these two modalities provide complimentary information. The challenges, however, are to develop effective methods to fuse the connectivity information from these two approaches.[126] Existing methods are mostly limited to *post hoc* analysis that either tests the functional connectivity between the two ends of a fiber bundle or the structural connectivity between functional ROIs, such as the nodes of default mode networks. For future development, more focus will be devoted to improving the structural connectomes with functional connectivity or vice versa. For example, one key question is the enhancement of the predictive power of functional connectivity with structural connectivity. The focus will be on tractography methods with reduced false positives and negatives such as the novel methods that aim to preserving the topographic regularity of fiber tracts.[111] Dynamic functional connectivity is another promising direction that holds the potential for detecting transient connectivity between brain regions.[127,128] This could boost the anatomical priors for computing structural connectivity. Besides function MRI, other imaging modalities can also improve the computation of structural connectivity. The myelin content from quantitative T2 can potentially be combined with the compartment modeling from multi-shell dMRI.[129,130]

Deep connectome phenotyping for brain imaging studies

With conventional DTI technology, major cortical bundles have been successfully reconstructed and widely used in various imaging studies. The high-resolution connectome imaging methods will no doubt improve the reliability and accuracy for these major bundles. Furthermore, the FOD-based tractography from connectome imaging data will enable the reconstruction of more detailed fascicles and allow us to generate a more complete description of systems such as the cortico–striato–thalamo–cortical network and the limbic system. Using connectome imaging, we have the opportunity to develop robust algorithms and software tools to systematically characterize the integrity of these circuits. In addition to in-depth modeling and quantification of these brain circuits, connectome-based parcellation[95,131,132] will produce whole-brain network models at much finer resolution than existing works. Together with multimodal fusion strategies, these connectome features will form a set of deep phenotypes for mining with genetic and behavioral data. This matches perfectly with current developments in Big Data and deep learning methods.[133]

CONFLICT OF INTEREST

The authors declare no conflict of interest.

ACKNOWLEDGMENTS

This work was in part supported by NIH Grants R01EB022744, K01EB013633, P41EB015922, U54EB020406 and R01MH094343.

REFERENCES

1 Ahmari SE, Spellman T, Douglass NL, Kheirbek MA, Simpson HB, Deisseroth K *et al.* Repeated cortico-striatal stimulation generates persistent OCD-like behavior. *Science* 2013; **340**: 1234–1239.
2 Burguière E, Monteiro P, Feng G, Graybiel AM. Optogenetic stimulation of lateral orbitofronto-striatal pathway suppresses compulsive behaviors. *Science* 2013; **340**: 1243–1246.
3 Haber SN. Corticostriatal circuitry. *Dialogues Clin Neurosci* 2016; **18**: 7–21.
4 Haber SN, Knutson B. The reward circuit: linking primate anatomy and human imaging. *Neuropsychopharmacology* 2010; **35**: 4–26.
5 Rolls ET. Limbic systems for emotion and for memory, but no single limbic system. *Cortex* 2015; **62**: 119–157.
6 Zingg B, Hintiryan H, Gou L, Song MY, Bay M, Bienkowski MS *et al.* Neural networks of the mouse neocortex. *Cell* 2014; **156**: 1096–1111.
7 Basser PJ, Mattiello J, LeBihan D. MR diffusion tensor spectroscopy and imaging. *Biophys J* 1994; **66**: 259–267.
8 Basser PJ, Jones DK. Diffusion-tensor MRI: theory, experimental design and data analysis - a technical review. *NMR Biomed* 2002; **15**: 456–467.
9 Mori S, Crain BJ, Chacko VP, Van Zijl PCM. Three-dimensional tracking of axonal projections in the brain by magnetic resonance imaging. *Ann Neurol* 1999; **45**: 265–269.
10 Basser PJ, Pajevic S, Pierpaoli C, Duda J, Aldroubi A. *In vivo* fiber tractography using DT-MRI data. *Magn Reson Med* 2000; **44**: 625–632.
11 van den Heuvel MP, Hulshoff Pol HE. Exploring the brain network: a review on resting-state fMRI functional connectivity. *Eur Neuropsychopharmacol* 2010; **20**: 519–534.
12 Van Dijk KRA, Hedden T, Venkataraman A, Evans KC, Lazar SW, Buckner RL. Intrinsic functional connectivity as a tool for human connectomics: theory, properties, and optimization. *J Neurophysiol* 2010; **103**: 297–321.
13 Biswal B, Yetkin FZ, Haughton VM, Hyde JS. Functional connectivity in the motor cortex of resting human brain using echo-planar MRI. *Magn Reson Med* 1995; **34**: 537–541.
14 Toga AW, Clark KA, Thompson PM, Shattuck DW, Van Horn JD. Mapping the human connectome. *Neurosurgery* 2012; **71**: 1–5.
15 Van Essen DC, Smith SM, Barch DM, Behrens TE, Yacoub E, Ugurbil K *et al.* The WU-Minn Human Connectome Project: an overview. *Neuroimage* 2013; **80**: 62–79.
16 Feinberg DA, Moeller S, Smith SM, Auerbach E, Ramanna S, Gunther M *et al.* Multiplexed echo planar imaging for sub-second whole brain FMRI and fast diffusion imaging. *PLoS ONE* 2010; **5**: e15710.
17 Moeller S, Yacoub E, Olman CA, Auerbach E, Strupp J, Harel N *et al.* Multiband multislice GE-EPI at 7 Tesla, with 16-fold acceleration using partial parallel imaging with application to high spatial and temporal whole-brain fMRI. *Magn Reson Med* 2010; **63**: 1144–1153.
18 Setsompop K, Gagoski BA, Polimeni JR, Witzel T, Wedeen VJ, Wald LL. Blipped-controlled aliasing in parallel imaging for simultaneous multislice echo planar imaging with reduced g-factor penalty. *Magn Reson Med* 2012; **67**: 1210–1224.
19 Setsompop K, Kimmlingen R, Eberlein E, Witzel T, Cohen-Adad J, McNab JA *et al.* Pushing the limits of *in vivo* diffusion MRI for the Human Connectome Project. *Neuroimage* 2013; **80**: 220–233.
20 Sotiropoulos SN, Jbabdi S, Xu J, Andersson JL, Moeller S, Auerbach EJ *et al.* Advances in diffusion MRI acquisition and processing in the Human Connectome Project. *Neuroimage* 2013; **80**: 125–143.
21 Ugurbil K, Xu J, Auerbach EJ, Moeller S, Vu AT, Duarte-Carvajalino JM *et al.* Pushing spatial and temporal resolution for functional and diffusion MRI in the Human Connectome Project. *Neuroimage* 2013; **80**: 80–104.
22 Toga AW, Foster I, Kesselman C, Madduri R, Chard K, Deutsch EW *et al.* Big biomedical data as the key resource for discovery science. *J Am Med Inform Assoc* 2015; **22**: 1126–1131.
23 Van Horn JD, Toga AW. Human neuroimaging as a "Big Data" science. *Brain Imaging Behav* 2014; **8**: 323–331.
24 Behrens TE, Sporns O. Human connectomics. *Curr Opin Neurobiol* 2012; **22**: 144–153.
25 Bullmore E, Sporns O. Complex brain networks: graph theoretical analysis of structural and functional systems. *Nat Rev Neurosci* 2009; **10**: 186–198.
26 Basser PJ, Özarslan E. Chapter 1 - Introduction to diffusion MRI. In: *Diffusion MRI*, 2nd edn. Academic Press: San Diego, CA, USA, 2014, pp 3–9.
27 Pipe J. Chapter 2 - Pulse sequences for diffusion-weighted MRI. In: *Diffusion MRI*, 2nd edn. Academic Press: San Diego, CA, USA, 2014, pp 11–34.
28 Tuch DS. Q-ball imaging. *Magn Reson Med* 2004; **52**: 1358–1372.
29 Wedeen VJ, Hagmann P, Tseng W-YI, Reese TG, Weisskoff RM. Mapping complex tissue architecture with diffusion spectrum magnetic resonance imaging. *Magn Reson Med* 2005; **54**: 1377–1386.
30 Jezzard P, Barnett AS, Pierpaoli C. Characterization of and correction for eddy current artifacts in echo planar diffusion imaging. *Magn Reson Med* 1998; **39**: 801–812.
31 Jezzard P, Clare S. Sources of distortion in functional MRI data. *Hum Brain Mapp* 1999; **8**: 80–85.
32 Rohde GK, Barnett AS, Basser PJ, Marenco S, Pierpaoli C. Comprehensive approach for correction of motion and distortion in diffusion-weighted MRI. *Magn Reson Med* 2004; **51**: 103–114.
33 Andersson JL, Sotiropoulos SN. Non-parametric representation and prediction of single- and multi-shell diffusion-weighted MRI data using Gaussian processes. *Neuroimage* 2015; **122**: 166–176.
34 Andersson JL, Sotiropoulos SN. An integrated approach to correction for off-resonance effects and subject movement in diffusion MR imaging. *Neuroimage* 2016; **125**: 1063–1078.
35 Jezzard P, Balaban RS. Correction for geometric distortion in echo planar images from B0 field variations. *Magn Reson Med* 1995; **34**: 65–73.
36 Andersson JLR, Skare S, Ashburner J. How to correct susceptibility distortions in spin-echo echo-planar images: application to diffusion tensor imaging. *Neuroimage* 2003; **20**: 870–888.
37 Holland D, Kuperman JM, Dale AM. Efficient correction of inhomogeneous static magnetic field-induced distortion in echo planar imaging. *Neuroimage* 2010; **50**: 175–183.
38 Irfanoglu MO, Modi P, Nayak A, Hutchinson EB, Sarlls J, Pierpaoli C. DR-BUDDI (Diffeomorphic Registration for Blip-Up blip-Down Diffusion Imaging) method for correcting echo planar imaging distortions. *Neuroimage* 2015; **106**: 284–299.
39 Norris DG. Implications of bulk motion for diffusion-weighted imaging experiments: effects, mechanisms, and solutions. *J Magn Reson Imaging* 2001; **13**: 486–495.
40 Skare S, Andersson JL. On the effects of gating in diffusion imaging of the brain using single shot EPI. *Magn Reson Imaging* 2001; **19**: 1125–1128.
41 Nunes RG, Jezzard P, Clare S. Investigations on the efficiency of cardiac-gated methods for the acquisition of diffusion-weighted images. *J Magn Reson* 2005; **177**: 102–110.
42 Andersson JL, Graham MS, Zsoldos E, Sotiropoulos SN. Incorporating outlier detection and replacement into a non-parametric framework for movement and distortion correction of diffusion MR images. *Neuroimage* 2016; **141**: 556–72.
43 Assaf Y, Basser PJ. Composite hindered and restricted model of diffusion (CHARMED) MR imaging of the human brain. *Neuroimage* 2005; **27**: 48–58.
44 Basser PJ, Mattiello J, LeBihan D. Estimation of the effective self-diffusion tensor from the NMR spin echo. *J Magn Reson B* 1994; **103**: 247–254.
45 Koay CG, Chang LC, Carew JD, Pierpaoli C, Basser PJ. A unifying theoretical and algorithmic framework for least squares methods of estimation in diffusion tensor imaging. *J Magn Reson* 2006; **182**: 115–125.
46 Basser PJ, Pierpaoli C. Microstructural and physiological features of tissues elucidated by quantitative-diffusion-tensor MRI. *J Magn Reson B* 1996; **111**: 209–219.
47 Nir TM, Jahanshad N, Villalon-Reina JE, Toga AW, Jack CR, Weiner MW *et al.* Effectiveness of regional DTI measures in distinguishing Alzheimer's disease, MCI, and normal aging. *Neuroimage Clin* 2013; **3**: 180–195.
48 Ringman JM, O'Neill J, Geschwind D, Medina L, Apostolova LG, Rodriguez Y *et al.* Diffusion tensor imaging in preclinical and presymptomatic carriers of familial Alzheimer's disease mutations. *Brain* 2007; **130**: 1767–1776.
49 Yassa MA, Muftuler LT, Stark CE. Ultrahigh-resolution microstructural diffusion tensor imaging reveals perforant path degradation in aged humans *in vivo*. *Proc Natl Acad Sci USA* 2010; **107**: 12687–12691.
50 Koch K, Reess TJ, Rus OG, Zimmer C, Zaudig M. Diffusion tensor imaging (DTI) studies in patients with obsessive-compulsive disorder (OCD): a review. *J Psychiatr Res* 2014; **54**: 26–35.
51 Kubicki M, Westin C-F, Maier SE, Frumin M, Nestor PG, Salisbury DF *et al.* Uncinate Fasciculus findings in schizophrenia: a Magnetic Resonance Diffusion Tensor Imaging Study. *Am J Psychiatry* 2002; **159**: 813–820.
52 Song SK, Sun SW, Ju WK, Lin SJ, Cross AH, Neufeld AH. Diffusion tensor imaging detects and differentiates axon and myelin degeneration in mouse optic nerve after retinal ischemia. *Neuroimage* 2003; **20**: 1714–1722.
53 Sun SW, Liang HF, Trinkaus K, Cross AH, Armstrong RC, Song SK. Noninvasive detection of cuprizone induced axonal damage and demyelination in the mouse corpus callosum. *Magn Reson Med* 2006; **55**: 302–308.
54 Tuch DS, Reese TG, Wiegell MR, Makris N, Belliveau JW, Wedeen VJ. High angular resolution diffusion imaging reveals intravoxel white matter fiber heterogeneity. *Magn Reson Med* 2002; **48**: 577–582.

55 Behrens TEJ, Berg HJ, Jbabdi S, Rushworth MFS, Woolrich MW. Probabilistic diffusion tractography with multiple fibre orientations: what can we gain? *Neuroimage* 2007; **34**: 144–155.
56 Peled S, Friman O, Jolesz F, Westin C-F. Geometrically constrained two-tensor model for crossing tracts in DWI. *Magn Reson Imaging* 2006; **24**: 1263–1270.
57 Anderson AW. Measurement of fiber orientation distributions using high angular resolution diffusion imaging. *Magn Reson Med* 2005; **54**: 1194–1206.
58 Tournier JD, Calamante F, Gadian DG, Connelly A. Direct estimation of the fiber orientation density function from diffusion-weighted MRI data using spherical deconvolution. *Neuroimage* 2004; **23**: 1176–1185.
59 Descoteaux M, Angelino E, Fitzgibbons S, Deriche R. Regularized, fast, and robust analytical Q-ball imaging. *Magn Reson Med* 2007; **58**: 497–510.
60 Dell'Acqua F, Scifo P, Rizzo G, Catani M, Simmons A, Scotti G *et al.* A modified damped Richardson–Lucy algorithm to reduce isotropic background effects in spherical deconvolution. *Neuroimage* 2010; **49**: 1446–1458.
61 Jian B, Vemuri BC. A unified computational framework for deconvolution to reconstruct multiple fibers from diffusion weighted MRI. *IEEE Trans Med Imaging* 2007; **26**: 1464–1471.
62 Descoteaux M, Deriche R, Knosche TR, Anwander A. Deterministic and probabilistic tractography based on complex fibre orientation distributions. *IEEE Trans Med Imaging* 2009; **28**: 269–286.
63 Patel V, Shi Y, Thompson PM, Toga AW. Mesh-based spherical deconvolution: a flexible approach to reconstruction of non-negative fiber orientation distributions. *Neuroimage* 2010; **51**: 1071–1081.
64 Tran G, Shi Y. Fiber orientation and compartment parameter estimation from multi-shell diffusion imaging. *IEEE Trans Med Imaging* 2015; **34**: 2320–2332.
65 Tournier JD, Calamante F, Connelly A. Robust determination of the fibre orientation distribution in diffusion MRI: non-negativity constrained super-resolved spherical deconvolution. *Neuroimage* 2007; **35**: 1459–1472.
66 Tran G, Shi Y. Adaptively constrained convex optimization for accurate fiber orientation estimation with high order spherical harmonics. *Med Image Comput Comput Assist Interv* 2013; **16**(Pt 3): 485–492.
67 Cheng J, Deriche R, Jiang T, Shen D, Yap P-T. Non-negative spherical deconvolution (NNSD) for estimation of fiber orientation distribution function in single-/multi-shell diffusion MRI. *Neuroimage* 2014; **101**: 750–764.
68 Yeh F-C, Wedeen VJ, Tseng W-YI. Estimation of fiber orientation and spin density distribution by diffusion deconvolution. *Neuroimage* 2011; **55**: 1054–1062.
69 Jbabdi S, Sotiropoulos SN, Savio AM, Grana M, Behrens TE. Model-based analysis of multishell diffusion MR data for tractography: how to get over fitting problems. *Magn Reson Med* 2012; **68**: 1846–1855.
70 Jeurissen B, Tournier J-D, Dhollander T, Connelly A, Sijbers J. Multi-tissue constrained spherical deconvolution for improved analysis of multi-shell diffusion MRI data. *Neuroimage* 2014; **103**: 411–426.
71 Panagiotaki E, Schneider T, Siow B, Hall MG, Lythgoe MF, Alexander DC. Compartment models of the diffusion MR signal in brain white matter: a taxonomy and comparison. *Neuroimage* 2012; **59**: 2241–2254.
72 Christiaens D, Reisert M, Dhollander T, Sunaert S, Suetens P, Maes F. Global tractography of multi-shell diffusion-weighted imaging data using a multi-tissue model. *Neuroimage* 2015; **123**: 89–101.
73 Reisert M, Mader I, Anastasopoulos C, Weigel M, Schnell S, Kiselev V. Global fiber reconstruction becomes practical. *Neuroimage* 2011; **54**: 955–962.
74 Mangin JF, Fillard P, Cointepas Y, Le Bihan D, Frouin V, Poupon C. Toward global tractography. *Neuroimage* 2013; **80**: 290–296.
75 Tournier JD, Calamante F, Connelly A. MRtrix: diffusion tractography in crossing fiber regions. *Int J Imaging Syst Technol* 2012; **22**: 53–66.
76 Mori S, Kaufmann WE, Davatzikos C, Stieltjes B, Amodei L, Fredericksen K *et al.* Imaging cortical association tracts in the human brain using diffusion-tensor-based axonal tracking. *Magn Reson Med* 2002; **47**: 215–223.
77 Catani M, Howard RJ, Pajevic S, Jones DK. Virtual *in vivo* interactive dissection of white matter fasciculi in the human brain. *Neuroimage* 2002; **17**: 77–94.
78 Wakana S, Jiang H, Nagae-Poetscher LM, van Zijl PC, Mori S. Fiber tract-based atlas of human white matter anatomy. *Radiology* 2004; **230**: 77–87.
79 Fischl B, Sereno MI, Dale AM. Cortical surface-based analysis. II: inflation, flattening, and a surface-based coordinate system. *Neuroimage* 1999; **9**: 195–207.
80 Patenaude B, Smith SM, Kennedy DN, Jenkinson M. A Bayesian model of shape and appearance for subcortical brain segmentation. *Neuroimage* 2011; **56**: 907–922.
81 Rohlfing T, Brandt R, Menzel R, Maurer CR. Evaluation of atlas selection strategies for atlas-based image segmentation with application to confocal microscopy images of bee brains. *Neuroimage* 2004; **21**: 1428–1442.
82 Sabuncu MR, Yeo BTT, Van Leemput K, Fischl B, Golland P. A generative model for image segmentation based on label fusion. *IEEE Trans Med Imaging* 2010; **29**: 1714–1729.
83 Hongzhi W, Suh JW, Das SR, Pluta JB, Craige C, Yushkevich PA. Multi-atlas segmentation with joint label fusion. *IEEE Trans Pattern Anal Mach Intell* 2013; **35**: 611–623.
84 Shi Y, Lai R, Wang DJ, Pelletier D, Mohr D, Sicotte N *et al.* Metric optimization for surface analysis in the Laplace-Beltrami embedding space. *IEEE Trans Med Imaging* 2014; **33**: 1447–1463.
85 Avants BB, Epstein CL, Grossman M, Gee JC. Symmetric diffeomorphic image registration with cross-correlation: evaluating automated labeling of elderly and neurodegenerative brain. *Med Image Anal* 2008; **12**: 26–41.
86 Kammen A, Law M, Tjan BS, Toga AW, Shi Y. Automated retinofugal visual pathway reconstruction with multi-shell HARDI and FOD-based analysis. *Neuroimage* 2016; **125**: 767–779.
87 O'Donnell LJ, Westin CF. Automatic tractography segmentation using a high-dimensional white matter atlas. *IEEE Trans Med Imaging* 2007; **26**: 1562–1575.
88 Jin Y, Shi Y, Zhan L, Gutman BA, de Zubicaray GI, McMahon KL *et al.* Automatic clustering of white matter fibers in brain diffusion MRI with an application to genetics. *Neuroimage* 2014; **100**: 75–90.
89 Calamante F, Tournier J-D, Jackson GD, Connelly A. Track-density imaging (TDI): super-resolution white matter imaging using whole-brain track-density mapping. *Neuroimage* 2010; **53**: 1233–1243.
90 Aydogan D, Shi Y. Track filtering via iterative correction of TDI topology. In: Navab N, Hornegger J, Wells W, Frangi A (eds). *Medical Image Computing and Computer-Assisted Intervention – MICCAI*, vol. 9349. Springer International Publishing: New York, NY, USA, 2015, pp 20–27.
91 Hagmann P, Kurant M, Gigandet X, Thiran P, Wedeen VJ, Meuli R *et al.* Mapping human whole-brain structural networks with diffusion MRI. *PLoS ONE* 2007; **2**: e597.
92 Sporns O. Small-world connectivity, motif composition, and complexity of fractal neuronal connections. *Biosystems* 2006; **85**: 55–64.
93 Sporns O. The human connectome: a complex network. *Ann NY Acad Sci* 2011; **1224**: 109–125.
94 Shattuck DW, Mirza M, Adisetiyo V, Hojatkashani C, Salamon G, Narr KL *et al.* Construction of a 3D probabilistic atlas of human cortical structures. *Neuroimage* 2008; **39**: 1064–1080.
95 Glasser MF, Coalson TS, Robinson EC, Hacker CD, Harwell J, Yacoub E *et al.* A multi-modal parcellation of human cerebral cortex. *Nature* 2016; **536**: 171–178.
96 Rubinov M, Sporns O. Complex network measures of brain connectivity: uses and interpretations. *Neuroimage* 2010; **52**: 1059–1069.
97 van den Heuvel MP, Sporns O. Rich-club organization of the human connectome. *J Neurosci* 2011; **31**: 15775–15786.
98 Yogarajah M, Focke NK, Bonelli S, Cercignani M, Acheson J, Parker GJM *et al.* Defining Meyer's loop-temporal lobe resections, visual field deficits and diffusion tensor tractography. *Brain* 2009; **132**: 1656–1668.
99 Ebeling U, Reulen HJ. Neurosurgical topography of the optic radiation in the temporal lobe. *Acta Neurochir* 1988; **92**: 29–36.
100 Sherbondy AJ, Dougherty RF, Napel S, Wandell BA. Identifying the human optic radiation using diffusion imaging and fiber tractography. *J Vis* 2008; **8**: 12–12.
101 Dreessen de Gervai P, Sboto-Frankenstein UN, Bolster RB, Thind S, Gruwel MLH, Smith SD *et al.* Tractography of Meyer's loop asymmetries. *Epilepsy Res* 2014; **108**: 872–882.
102 Nieuwenhuys R, Voogd J, Cv Huijzen. *The Human Central Nervous System*, 4th edn. Springer: New York, USA, 2008, pp 967.
103 Paxinos G, Huang X, Sengul G, Watson C. Organization of brainstem nuclei. In: *The Human Nervous System*. 3rd edn. Elsevier Academic Press: Amsterdam, 2012, pp 260–327.
104 Trillo L, Das D, Hsieh W, Medina B, Moghadam S, Lin B *et al.* Ascending monoaminergic systems alterations in Alzheimer's disease. Translating basic science into clinical care. *Neurosci Biobehav Rev* 2013; **37**: 1363–1379.
105 Meola A, Yeh FC, Fellows-Mayle W, Weed J, Fernandez-Miranda JC. Human connectome-based tractographic atlas of the brainstem connections and surgical approaches. *Neurosurgery* 2016; **79**: 437–455.
106 van Baarsen KM, Kleinnijenhuis M, Jbabdi S, Sotiropoulos SN, Grotenhuis JA, van Cappellen van Walsum AM. A probabilistic atlas of the cerebellar white matter. *Neuroimage* 2016; **124**(Pt A): 724–732.
107 Edlow BL, McNab JA, Witzel T, Kinney HC. The structural connectome of the human central homeostatic network. *Brain Connect* 2015; **6**: 187–200.
108 Glasser MF, Rilling JK. DTI tractography of the human brain's language pathways. *Cereb Cortex* 2008; **18**: 2471–2482.
109 Catani M, Jones DK, Ffytche DH. Perisylvian language networks of the human brain. *Ann Neurol* 2005; **57**: 8–16.
110 Yagmurlu K, Middlebrooks EH, Tanriover N, Rhoton AL Jr. Fiber tracts of the dorsal language stream in the human brain. *J Neurosurg* 2016; **124**: 1396–1405.
111 Aydogan DB, Shi Y. Probabilistic tractography for topographically organized connectomes. In: Ourselin S, Joskowicz L, Sabuncu M, Unal G, Wells W (eds). Medical Image Computing and Computer-Assisted Intervention – MICCAI 2016: *19th International Conference, Proceedings, Part I* 2016; 17–21 October 2016: Athens, Greece. Springer: Cham, 2016, pp 201–209.

112 Vu AT, Auerbach E, Lenglet C, Moeller S, Sotiropoulos SN, Jbabdi S *et al.* High resolution whole brain diffusion imaging at 7 T for the Human Connectome Project. *Neuroimage* 2015; **122**: 318–331.
113 Stanisz GJ, Wright GA, Henkelman RM, Szafer A. An analytical model of restricted diffusion in bovine optic nerve. *Magn Reson Med* 1997; **37**: 103–111.
114 Assaf Y, Blumenfeld-Katzir T, Yovel Y, Basser PJ. Axcaliber: a method for measuring axon diameter distribution from diffusion MRI. *Magn Reson Med* 2008; **59**: 1347–1354.
115 Alexander DC, Hubbard PL, Hall MG, Moore EA, Ptito M, Parker GJM *et al.* Orientationally invariant indices of axon diameter and density from diffusion MRI. *Neuroimage* 2010; **52**: 1374–1389.
116 Zhang H, Schneider T, Wheeler-Kingshott CA, Alexander DC. NODDI: practical *in vivo* neurite orientation dispersion and density imaging of the human brain. *Neuroimage* 2012; **61**: 1000–1016.
117 Engel SA, Glover GH, Wandell BA. Retinotopic organization in human visual cortex and the spatial precision of functional MRI. *Cereb Cortex* 1997; **7**: 181–192.
118 Ruben J, Schwiemann J, Deuchert M, Meyer R, Krause T, Curio G *et al.* Somatotopic organization of human secondary somatosensory cortex. *Cereb Cortex* 2001; **11**: 463–473.
119 Schmahmann JD, Pandya DN, Wang R, Dai G, D'Arceuil HE, de Crespigny AJ *et al.* Association fibre pathways of the brain: parallel observations from diffusion spectrum imaging and autoradiography. *Brain* 2007; **130**(Pt 3): 630–653.
120 Jbabdi S, Lehman JF, Haber SN, Behrens TE. Human and monkey ventral prefrontal fibers use the same organizational principles to reach their targets: tracing versus tractography. *J Neurosci* 2013; **33**: 3190–3201.
121 Donahue CJ, Sotiropoulos SN, Jbabdi S, Hernandez-Fernandez M, Behrens TE, Dyrby TB *et al.* Using diffusion tractography to predict cortical connection strength and distance: a quantitative comparison with tracers in the monkey. *J Neurosci* 2016; **36**: 6758–6770.
122 Oh SW, Harris JA, Ng L, Winslow B, Cain N, Mihalas S *et al.* A mesoscale connectome of the mouse brain. *Nature* 2014; **508**: 207–214.
123 Calabrese E, Badea A, Cofer G, Qi Y, Johnson GA. A diffusion MRI tractography connectome of the mouse brain and comparison with neuronal tracer data. *Cereb Cortex* 2015; **25**: 4628–37.
124 Chen H, Liu T, Zhao Y, Zhang T, Li Y, Li M *et al.* Optimization of large-scale mouse brain connectome via joint evaluation of DTI and neuron tracing data. *Neuroimage* 2015; **115**: 202–213.
125 Wang Y, Wang Q, Haldar JP, Yeh FC, Xie M, Sun P *et al.* Quantification of increased cellularity during inflammatory demyelination. *Brain* 2011; **134**(Pt 12): 3590–3601.
126 Zhu D, Zhang T, Jiang X, Hu X, Chen H, Yang N *et al.* Fusing DTI and fMRI data: a survey of methods and applications. *Neuroimage* 2014; **102**(Part 1): 184–191.
127 Calhoun Vince D, Miller R, Pearlson G, Adalı T. The chronnectome: time-varying connectivity networks as the next frontier in fMRI data discovery. *Neuron* 2014; **84**: 262–274.
128 Hindriks R, Adhikari MH, Murayama Y, Ganzetti M, Mantini D, Logothetis NK *et al.* Can sliding-window correlations reveal dynamic functional connectivity in resting-state fMRI? *Neuroimage* 2016; **127**: 242–256.
129 MacKay A, Laule C, Vavasour I, Bjarnason T, Kolind S, Mädler B. Insights into brain microstructure from the T2 distribution. *Magn Reson Imaging* 2006; **24**: 515–525.
130 Deoni SC, Mercure E, Blasi A, Gasston D, Thomson A, Johnson M *et al.* Mapping infant brain myelination with magnetic resonance imaging. *J Neurosci* 2011; **31**: 784–791.
131 Behrens TE, Johansen-Berg H, Woolrich MW, Smith SM, Wheeler-Kingshott CA, Boulby PA *et al.* Non-invasive mapping of connections between human thalamus and cortex using diffusion imaging. *Nat Neurosci* 2003; **6**: 750–757.
132 Mars RB, Jbabdi S, Sallet J, O'Reilly JX, Croxson PL, Olivier E *et al.* Diffusion-weighted imaging tractography-based parcellation of the human parietal cortex and comparison with human and macaque resting-state functional connectivity. *J Neurosci* 2011; **31**: 4087–4100.
133 LeCun Y, Bengio Y, Hinton G. Deep learning. *Nature* 2015; **521**: 436–444.